AJNR

Radiologic-pathologic correlation: intracranial astrocytoma.

M Castillo, J H Scatliff, T W Bouldin and K Suzuki

AJNR Am J Neuroradiol 1992, 13 (6) 1609-1616
http://www.ajnr.org/content/13/6/1609.citation

Radiologic-Pathologic Correlation:
Intracranial Astrocytoma

Mauricio Castillo, James H. Scatliff, Thomas W. Bouldin, and Kinuko Suzuki

From the Departments of Radiology, Section of Neuroradiology (MC, JHS), and Pathology, Section of Neuropathology (TWB, KS), University of North Carolina School of Medicine, Chapel Hill, NC

Clinical History

An 8-year-old boy presented with progressive left lower extremity weakness of 2-weeks duration. Past medical history was unremarkable. Contrast-enhanced computed tomography (CT) demonstrated an enhancing mass in high right parietal convexity. An open biopsy revealed low-grade astrocytoma. Steroids and anticonvulsant medications were prescribed and the patient was discharged. One month later, he was readmitted due to increasing left-sided paresis. Physical examination showed weakness in the left lower and upper extremities as well as a left abducens palsy. Repeat contrast-enhanced CT showed interval development of low-attenuation regions in the center of the mass. Results of second open biopsy were again consistent with low-grade astrocytoma. Radiation therapy was started but hydrocephalus developed requiring placement of a ventriculoperitoneal shunt. The patient was readmitted 2 months later because of increasing lethargy, anorexia, and generalized weakness. Physical examination also revealed meningismus. Repeat contrast-enhanced CT and magnetic resonance (MR) showed that the tumor had extended into the left cerebral hemisphere via the corpus callosum (Figs. 1A and 1B). Supportive treatments were continued but the patient died 2 weeks later. Postmortem examination revealed a right hemispheric glioblastoma multiforme that had extended to the left hemisphere via the corpus callosum (Figs. 1C and 1D). The ependyma of the left lateral and third ventricles contained tumor cells. The meninges were thickened and fibrotic and showed tumor infiltration. Microscopical foci of tumor within perivascular spaces were also present in the pons near the abducens nuclei and in the upper cervical spinal cord. The meninges in the remaining spinal cord and cauda equina were also infiltrated by tumor.

General

Primary cerebral gliomas comprise 40%–60% of adult intracranial tumors (1). In adults, only a small percentage of gliomas are infratentorial, whereas 70%–80% of gliomas seen in children occur in the cerebellum (1). Supratentorial gliomas are found more frequently in males (3:2) during the 6th and 7th decades of life (peak incidence: 50 years of age) (1). Most adult supratentorial gliomas are forms of astrocytomas. The most malignant form of astrocytoma (glioblastoma multiforme) has an unfavorable prognosis, with most patients surviving less than 15 months after the initial diagnosis regardless of the mode of treatment (2). The average survival rate for the lower grade astrocytomas varies from 2.5 to 5 years after diagnosis (this does not include oligodendrogliomas).

Pathology

Histology

Astrocytomas are composed of neoplastic astrocytes (3). Histologically, they range from well-differentiated to undifferentiated; when

Address reprint requests to Mauricio Castillo, MD, Department of Radiology, CB# 7510, 217 Third Floor Old Infirmary, University of North Carolina at Chapel Hill, Chapel Hill, NC 27599-7510.

Index terms: Astrocytoma; Radiologic-pathologic correlations

AJNR 13:1609–1616, Nov/Dec 1992 0195-6108/92/1306-1609

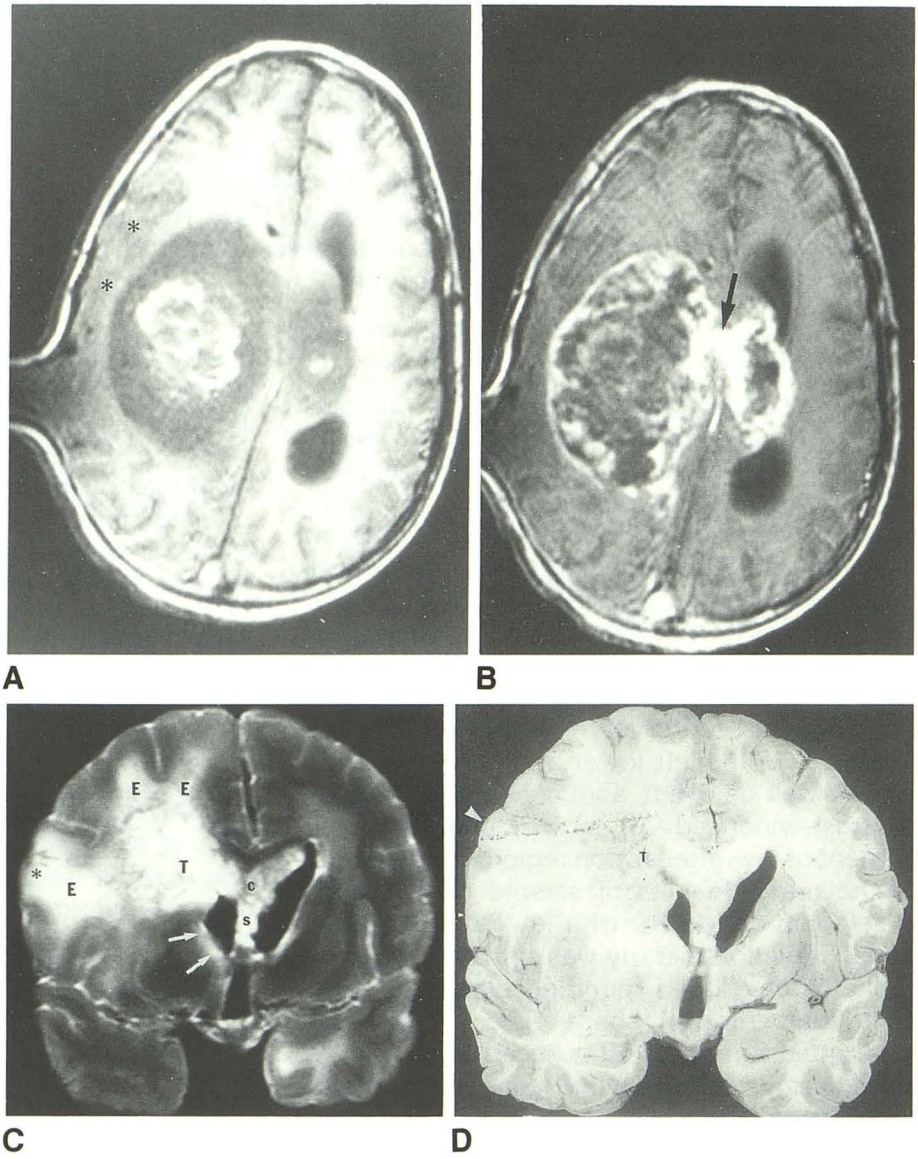

Fig. 1. *A*, Axial noncontrast MR T1-weighted image shows a large mass in the right hemisphere. The periphery of this mass is of low signal intensity. The central area of high signal intensity (also present on T2-weighted images) is presumed to represent hemorrhage (methemoglobin). There is compression of the right lateral ventricle and mild midline shift. A second smaller mass is present in the medial left hemisphere. This mass is mainly of low signal intensity and contains a central focus of hemorrhage. Intratumoral hemorrhage is more commonly seen in high-grade gliomas. The left lateral ventricle is mildly dilated secondary to entrapment of its frontal and occipital horns by tumor. The gray matter (*) overlying the right-sided mass is thickened and the gray-white junction is not clearly seen. The latter findings suggest the presence of either cortical edema and/or tumor infiltration. The right-sided artifact is secondary to a cerebrospinal fluid shunt.

B, Axial T1-weighted image after gadolinium administration at the same level as *A*. There is irregular and nodular enhancement of the periphery of both masses. Enhancing tumor is noted crossing the midline compatible with transcallosal extension (*arrow*). High-grade gliomas classically spread through white matter tracts such as the corpus callosum. This appearance represents the so-called "butterfly" glioma. The irregular pattern of enhancement also suggests the high-grade histology of this tumor.

C, Postmortem coronal T2-weighted image of the fixed brain in the same patient obtained 1 month after the studies shown in *A* and *B*. The bulk of the tumor (*T*) is seen as an area of high signal intensity. There is white matter edema (*E*) with its characteristic "finger-like" extensions into the subcortical regions. Tumor cells were found in these latter regions illustrating the lack of sensitivity of MR to exactly delineate the true margins of the tumor. Gray matter signal abnormality (as seen in *A*) is present in the right frontoparietal area near the operculum (*) and, pathologically, this region of cortex contained both areas of tumor invasion and areas of reactive edema. Clearly seen is tumor extending through the corpus callosum (*C*) which is of high signal intensity and is thickened. The tumor also infiltrates the septum pellucidum (*S*). An irregular area of high signal intensity is also seen in the outer wall of the right lateral ventricle (*arrows*) and subependymal tumor spread was found in this region. Subependymal spread may occur (as in this case) with high-grade gliomas. Although meningeal spread was diffusely present at autopsy, that feature is not appreciated in this image. Meningeal invasion represents another avenue for extension of high-grade gliomas. The high signal intensity in the left temporal lobe represents an artifact of fixation,.

D, Coronal section of the fixed brain at the same level as *C*. The large glioblastoma multiforme (*T*) abutting the lateral ventricle is clearly seen. There is infiltration and thickening of the septum pellucidum and the corpus callosum. There is invasion of the gray matter (*arrowhead*) laterally as seen on the MR image.

the astrocytes resemble normal ones they can be considered well-differentiated. Anaplastic changes are very common in astrocytomas, and include nuclear and cellular pleomorphism, vascular endothelial proliferation, and areas of tumor necrosis (4). Malignant astrocytomas show foci of anaplasia; glioblastomas are astrocytomas with foci of anaplasia and necrosis (3, 5). It is now generally accepted that tumor grading should be based on the most malignant portion present; however, the small tissue sample generally obtained by needle biopsy may not be representative of the more malignant regions of the mass. In many institutions the neurosurgeon obtains multiple biopsies at different tumor regions to minimize errors in pathologic grading. Approximately 80% of low-grade gliomas "dedifferentiate" into more aggressive forms (4). In general, more anaplastic elements are found in the center of higher grade tumors, while their periphery contains better differentiated cells; therefore, malignant gliomas can be of two types: those that arose from a benign astrocytoma, and those originating de novo.

To simplify tumor grading, the term "astrocytoma" refers to the old astrocytoma grades I and II (3). The terms "malignant" or "anaplastic" astrocytoma are used for the old astrocytoma grade III, and refer to a tumor of intermediate malignancy (3). "Glioblastoma multiforme" refers to the old astrocytoma grade IV (3). The term "multiforme" reflects the diverse appearance of the highly malignant cells that constitute these tumors.

Glial fibrillary acidic protein is a biochemically and immunologically distinct protein specific for astrocytes (6). Immunohistochemical tests to detect this marker are available and help to confirm the astrocytic nature of a tumor. The amount of glial fibrillary acidic protein present in an astrocytoma decreases as malignancy progresses (due to the presence of poorly differentiated cells).

Locations

Cerebral Hemispheres

The cerebral hemispheres are the most commonly involved site in adults (1). Anaplasia is found in approximately 80% of hemispheric astrocytomas (3, 4). Hemispheric low-grade gliomas are more commonly seen in younger patients. Although any part of the cerebrum may be involved, the frontal and temporal lobes are more commonly affected (2). There is relative sparing of the occipital regions (7). Involvement of central and deep structures such as the corpus callosum is not uncommon. When the corpus callosum is involved, bihemispheric invasion is generally present.

Cerebellum

The cerebellum is predominantly involved in children and adolescents. Cerebellar astrocytomas constitute approximately 16% of all brain tumors in these age groups (3). These gliomas are generally cystic (60%–80%) and of low-grade malignancy (pilocytic astrocytomas) (1). Many cystic gliomas may be totally resected and the patient may be considered cured. Overall survival rates at 20 years vary between 70%–80% (8).

Brainstem

Although brain stem astrocytoma occurs more commonly in children, it may also be found in adults. Brain stem gliomas comprise approximately 20% of all posterior fossa gliomas in children (9). These tumors are diffusely infiltrating and may extend into the medulla, midbrain, thalamus, or be exophytic. Anaplastic features are seen in up to 60% of these malignancies (3, 4). Occasionally, brain stem gliomas may demonstrate preferential growth into the fourth ventricle. Clinically and by imaging, brain stem gliomas may mimic pontine encephalitis.

Hypothalamus-Optic Chiasm

These tumors represent 1%–2% of adult gliomas and approximately 3% of childhood gliomas (10). At diagnosis, most tumors are large and their epicenter cannot be reliably located (10). Moreover, 50% of all "optic" gliomas appear to originate from the hypothalamus (3). Although these tumors are slow growing, they are microscopically infiltrating and may compress or fill the third ventricle

leading to hydrocephalus. The behavior of the larger tumors is unpredictable and they are less responsive to radiation therapy than gliomas confined to the optic nerves (10).

Special Forms

Associated with Neurofibromatosis

Optic nerve gliomas are present in 30%–90% of patients with neurofibromatosis type I (NFI) (11). However, optic nerve glioma may occur in an isolated fashion. More than 75% of optic nerve gliomas are found in children less than 12 years of age (3). Bilateral tumors are seen in 10%–20% of cases, especially patients with NFI (3). The majority arise in the optic nerve and extend posteriorly. These gliomas may also arise from the retina or from the optic chiasm or hypothalamus. Ten to 15% of patients with NFI have tumors arising directly from the chiasm-hypothalamus regions, thalamus, basal ganglia, brain stem, and cerebral hemispheres (11). Patients with optic nerve gliomas have a good prognosis for life but a poor prognosis for vision. These tumors are generally classified as pilocytic astrocytomas.

Gliomatosis Cerebri

This term is applied to a very rare type of disseminated astrocytic neoplasia with no grossly discernible focal masses (3). The peak incidence is between 20–40 years of age. The clinical presentation is nonspecific and nonfocal. Signs and symptoms are relatively mild in relation to the degree of tumor extent (12). The cerebral hemispheres are more commonly involved, but the tumor may be found in the cerebellum and brain stem. The gray and white matter are both involved (13). By MR and CT, the underlying cerebral structures are relatively preserved.

Leptomeningeal

Gliomas arising from the meninges with no parenchymal foci are extremely rare and are speculated to arise from ectopic glial nodules within the leptomeninges (4).

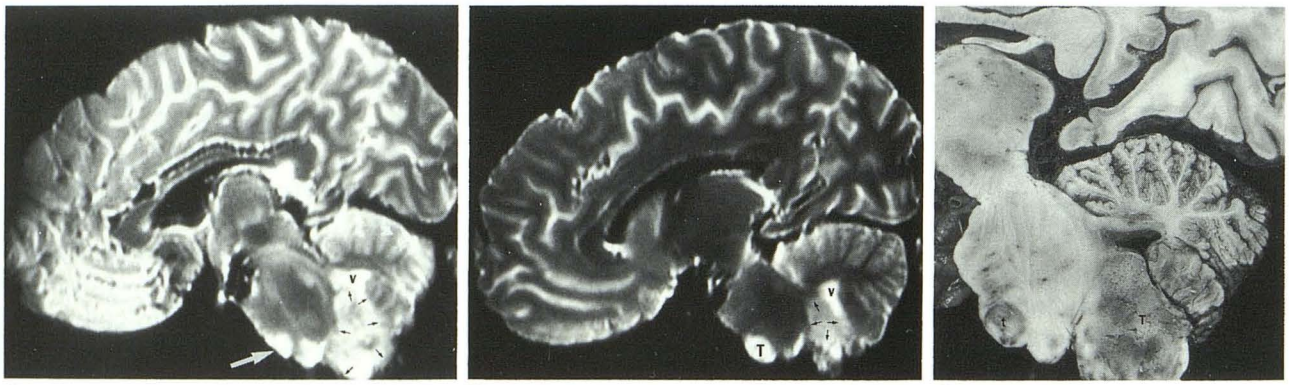

Fig. 2. *A*, Midsagittal postmortem T2-weighted image in a 13-year-old boy who presented 2 years previously with diplopia and headache and was treated with radiation therapy at an outside institution. There is a discreet focus (*large arrow*) of high signal intensity in the lower pons. The lower pontine area of signal abnormality is believed to represent an artifact of fixation as no discreet tumor focus was found at that level. The right cerebellar tonsil (*small arrows*) is markedly enlarged and is also of high signal intensity. The fourth ventricle (*V*) is displaced rostrally by the mass. (Premortem MR not performed.)

B, Right parasagittal postmortem T2-weighted image shows a discreet and well-defined focus (*T*) of abnormal high signal intensity in the lower ventral pons. Enlargement and abnormal increased signal intensity from the cerebellar tonsil (*arrows*) is again seen. The fourth ventricle (*V*) is displaced rostrally. Note that the tissues separating both lesions are of normal signal intensity. Despite this finding, microscopical examination revealed tumor cells in between both lesions (multifocal glioma) and the features of all lesions were compatible with glioblastoma multiforme.

C, Midsagittal section of the fixed specimen corresponding to *A* and *B*. The cerebellar tonsil (*T*) harbors a malignant glioma and is diffusely enlarged. A separate tumor nodule (*t*) is present in the low pons. Despite the grossly normal appearance of tissues between these tumors, diffuse infiltration was present at microscopy at these levels, communicating both tumors and, thus, making the diagnosis of multifocal glioblastoma multiforme.

Multifocal and Multicentric

The incidence of multiple gliomas ranges from 0.5%–10% (14). Multiple gliomas may be synchronous (occurring at the same time) or metachronous (occurring at different times). Lesions that have parenchymal connections or have spread through the cerebrospinal fluid pathways are termed multifocal (Fig. 2) (3). Isolated gliomas with no microscopical continuity may occur and are termed "multicentric" (Figs. 3–5) (3). Distinguishing them from the more common metastases to the brain may not be entirely possible radiographically. The presence of multiple, solid, and enhancing lesions located in the deep parenchyma and involving only one cerebral hemisphere should raise the possibility of multiple gliomas (15).

Imaging

CT

On noncontrast CT studies the majority of gliomas are seen as areas of low density (18–30 HU) (Figs. 3A and 3B) (16). They may also contain patchy regions of density similar to that of normal brain. Normal noncontrast CT studies are not rare (2). The margins of the lesion are ill-defined and merge imperceptibly with the neighboring normal brain (Fig. 3B). At times, the tumor margins may be slightly hyperdense. This finding may reflect hemorrhage, cellular compactness, compressed normal brain tissues, or simply appear this way due to low density of the surrounding edema. Mass effect and shift of midline structures may also be present. The presence of hydrocephalus varies and can be considered a late finding in brain stem gliomas, but may also occur early as seen in gliomas arising in the region of the third ventricle. Administration of iodinated contrast material is necessary to better delineate these lesions. Although the pattern of contrast enhancement does not always predict the histologic grade, an educated guess is possible in the many cases (17). Low-grade gliomas generally show little or no enhancement. This imaging feature reflects an intact or relatively intact blood brain barrier (BBB). Patchy areas of contrast enhancement may be present in up to 40% of low-grade gliomas (2). The margins of low-grade tumors are generally poorly defined (Fig. 3A). Calcifications occur in 10%–20% of gliomas, generally those of low-grade malignancy (Figs. 4A and 4B). Calcifications may have any appearance, and their presence does not preclude a high-grade glioma.

Cerebellar pilocytic astrocytomas deserve special mention because of their characteristic imaging features. Although the majority of these tumors occur in the cerebellum, they are also be found in the region of the chiasm/hypothalamus/third ventricle and in the cerebral hemispheres (18). Pilocytic gliomas are sharply demarcated and lobular. Approximately two thirds are cystic and the majority show marked peripheral and, at times, nodular contrast enhancement (Fig. 5) (1). Edema and tumor calcifications are absent.

Anaplastic gliomas and glioblastoma multiforme generally show rim enhancement. The rim is nodular, thick, irregular, and hyperdense reflecting the breakdown of the BBB at those levels (Fig. 3A). However, minimal or no enhancement at all may be occasionally present in high-grade tumors (Fig. 3B) (19, 20). A central portion of low density is seen in up to 95% of glioblastoma multiforme and reflects necrosis and/or cyst formation (3). Edema tracking along white matter pathways is commonly present (75%–90% of cases) (Figs. 3A and 3B) (1). Different patterns of mass effect and herniations can be seen and may vary according to the location of the tumor. Hemorrhage occurs more often in the higher grade gliomas. Hemorrhage may be the presenting event in a patient without a known tumor. Gliomas extend along the white matter tracts. Although they may arise initially in one hemisphere, high-grade tumors may become bihemispheric by crossing through central white matter tracts such as the corpus callosum ("butterfly" glioma) and the anterior and posterior commissures (Figs. 1A–1D). Infiltrating brain-stem gliomas may extend into the cerebellar hemispheres. Ventricular extension due to infiltration to the ependymal surfaces may occur and represents a grave prognostic sign (Figs. 1A–1D). If multiple enhancing masses are encountered on a contrast-enhanced CT study, there is no way to distinguish multifocal glioma from more common processes such as metastases or lymphoma (Figs. 2–5).

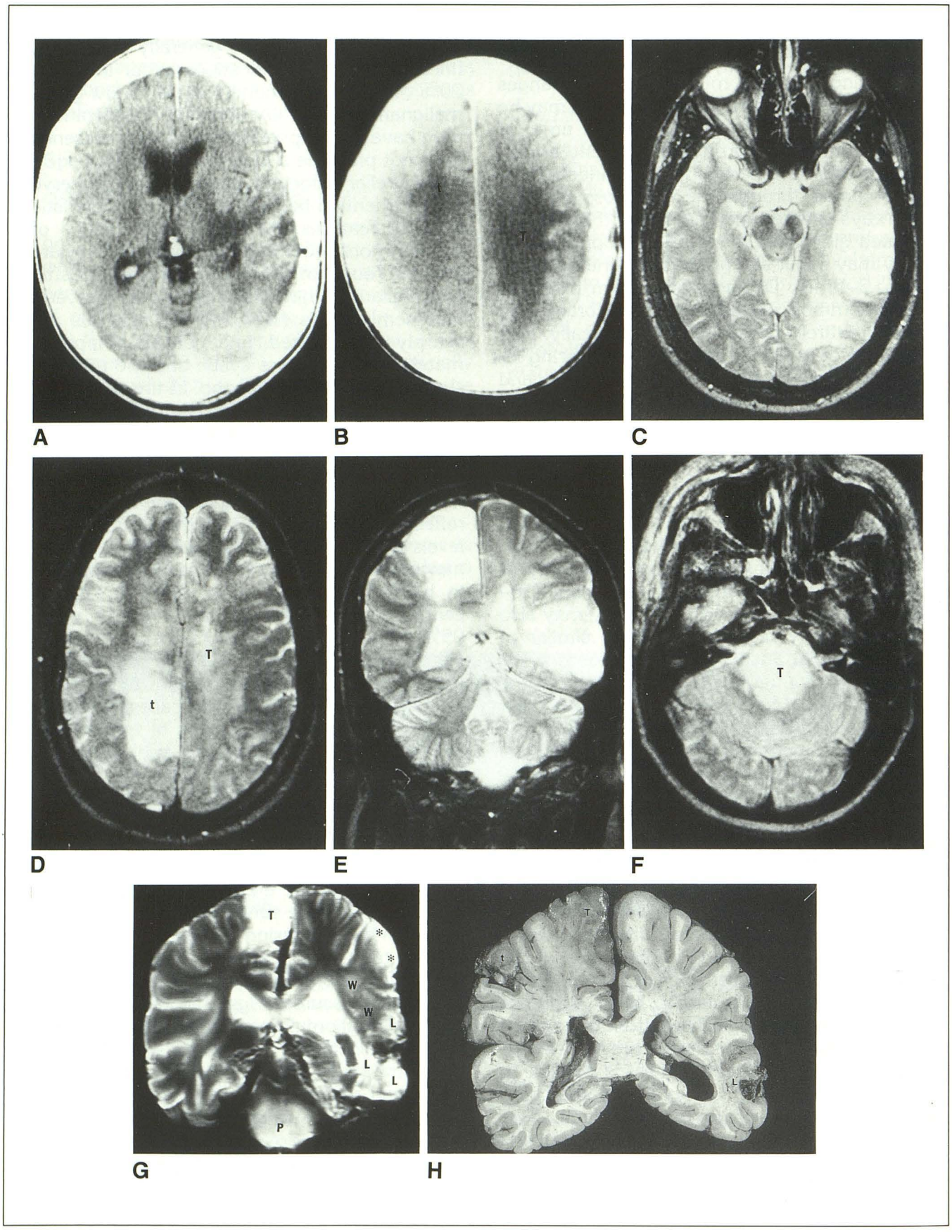
A
B
C
D
E
F
G
H
T
t
W
L
P

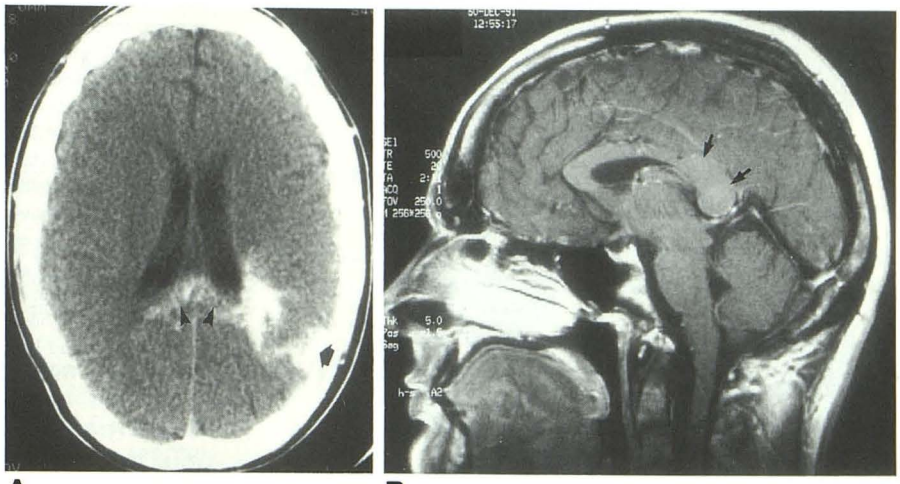

A B

Fig. 4. *A*, Noncontrast CT section in a patient with an extensively calcified glioblastoma multiforme arising in the left parietal occipital region. This tumor had not received any radiation at the time of this study. Laterally, the tumor (*arrow*) invades the cortex and it extends medially (*arrowheads*) along the splenium of the corpus callosum.

B, Midsagittal T1-weighted image after gadolinium administration in the same patient as *A*. Note the enlarged corpus callosum posteriorly (*arrows*) secondary to tumor infiltration of this white matter tract.

MR

The MR findings closely resemble those seen by CT. MR defines the extent of the lesion better than CT. However, tumor may be present beyond the abnormal regions seen on MR (Figs. 3C and 3D) (17). Conversely, the extent of tumor in remission may be overestimated on MR T2-weighted images due to the high

Fig. 3. *A*, Axial CT section after contrast administration in a 33-year-old man who presented with seizures and difficulty talking. The lesion in the left temporal region shows irregular and somewhat nodular enhancement. There is surrounding edema and mild compression of the ipsilateral ventricle.

B, Contrast-enhanced axial CT section in the same patient shows areas of low density in the left centrum semiovale (*T*) and in the right high parietal region (*t*). This appearance is that of the classic "vasogenic" edema configuration, and despite the absence of definite areas of contrast enhancement, tumor was present on both sites.

C, Axial T2-weighted image obtained 1 month after *A* and *B*. During the interval, the patient underwent radiation therapy and intra-arterial infusion of cisplatin. There is extensive abnormal high signal intensity on the left temporal and occipital lobes, suggesting edema. Although discreet tumor foci are not identifiable amid the edema, pathology showed a well-defined tumor focus along the most lateral aspect of this abnormality (where no normal gray matter is seen).

D, Axial T2-weighted image caudal to *B* shows interval decrease in size of the zone of edema previously seen in left centrum semiovale (*T*). Again noted is the abnormal signal intensity as seen in the right parietal region (*t*). Notice the absence of identifiable discreet tumor foci in both lesions. No gadolinium was administered for this study.

E, Coronal T2-weighted image shows the zones of abnormal high signal intensity in the right parietal and left temporal lobes. Notice that the signal abnormalities in both lesions extend to involve gray matter. Microscopy revealed direct extension of the tumor into the cortex at both sites. The meninges overlying the left temporal lesion were also infiltrated by tumor (not appreciated by MR).

F, Axial T2-weighted image obtained 3 weeks after the study shown in *C–E*. At this time, the patient had developed dysphagia, dyspnea, and progressive lethargy. The supratentorial lesions were stable but a new area of abnormal high signal intensity (*T*) developed in the pons. No gadolinium was given due to lack of venous access. Despite supportive treatment the patient died 2 days after this study.

G, Postmortem coronal T2-weighted image at a comparable level to *E* shows diffuse high signal intensity from the tumor (*T*) in the right parietal lobe. By pathology, two tumor foci were present in the medical and superior aspects of this lesion. Notice that the gray matter superior and medial is infiltrated. Tumor infiltration of the cortex and white matter was histologically present but not obvious on the MR studies. Abnormal high signal is also present in the pons (*P*) and the left temporal lobe (*L*). Discreet separation between zones of edema and tumor cannot be made on this study. The white matter (*W*) in the temporal lobe shows subtle but definite abnormal increased signal intensity probably related to radiation and/or chemotherapy. No tumor cells were present in this latter area. A fourth area of abnormal signal intensity (involving both gray and white matter) (*) is seen in the left temporoparietal region. Microscopy revealed tumor at this level. All lesions were compatible with glioblastoma multiforme and showed no communication between them, thus making this a multicentric tumor. In this case, both synchronous and metachronous lesions occurred.

H, Coronal section of the fixed specimen corresponding to *E* and *G*. The large glioblastoma multiforme (*T*) in the superior right parietal lobe clearly infiltrates gray matter as seen on MR. A second and totally separate glioblastoma multiforme (*t*) is present laterally and inferiorly. The tumor (*L*) in the left temporal region also infiltrates the cortex.

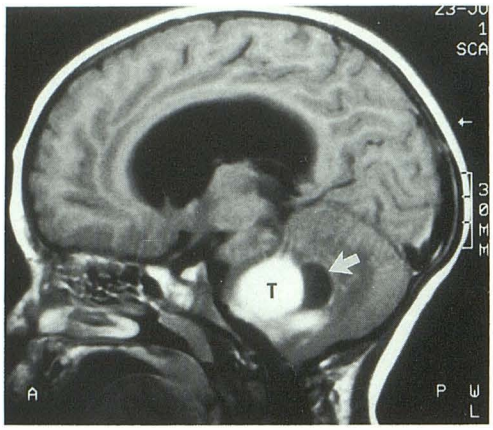

Fig. 5. Parasagittal post-gadolinium T1-weighted image showing marked enhancement of the solid portion (*T*) of this pilocytic astrocytoma. The cyst (*arrow*) located dorsally, does not enhance.

signal intensity of surrounding edema and/or radiation-induced changes (21). Calcifications may not be appreciated if only spin-echo techniques are utilized (22). On nonenhanced T1-weighted images these tumors are of low signal intensity (Fig. 1A). T2-weighted images show the tumor and surrounding edema to be of high signal intensity (reflecting high water content in both) (Figs. 3C–3F). Therefore, on T2-weighted images, tumor and edema may not be separable from each other. In our experience, involvement of the gray matter strongly correlates with the presence of tumor. Like iodinated contrast media, gadolinium enhancement depends upon disruption of the BBB. The enhancement patterns seen after gadolinium administration are similar to those previously described for contrast-enhanced CT with high-grade tumors showing greater enhancement than their more benign counterparts (21, 23) (Figs. 1A and 1B). Following the administration of gadolinium, maximum enhancement occurs during the first 15 minutes. Hemorrhage may also be identified by MR. Subpial tumor spread and tumor in the subarachnoid space is not commonly identified by MR (21).

References

1. Atlas SW. Intra-axial brain tumors: In: Atlas SW, ed. *Magnetic resonance imaging of the brain and spine*. New York: Raven, 1991:249–264
2. Latchaw RE, Johnson DW, Kanal E. Primary intracranial tumors: neuroepithelial tumors, sarcomas, and lymphomas. In: Latchaw RE, ed. *MR and CT imaging of the head, neck, and spine*. St. Louis: Mosby, 1991:450–471
3. Okazaki H. *Fundamentals of neuropathology*. 2nd ed. New York: Igaku-Shoin, 1989:204–219
4. Russell DS, Rubinstein LJ. *Pathology of tumors of the nervous systems*, 5th ed. Baltimore: Williams & Wilkins, 1989
5. Burger PC, Scheithaver BW, Vogel FS. *Surgical pathology of the brain and its coverings*. 3rd ed. New York: Churchill Livingstone, 1991
6. Schiffer D, Giordana MT, Mauro A, Migheli A. Glial fibrillary acidic protein (GFAP) in human cerebral tumors: an immunohistochemical study. *Tumori* 1983;69:95–104
7. Mckeran RO, Thomas DGT. The clinical study of gliomas. In: Thomas DGT, Graham DI, eds. *Brain tumors: scientific basis, clinical investigation and current therapy*. London: Butterworths, 1980:194
8. Wallner KE, Gonzales MF, Edwards MSB, et al. Treatment results of juvenile pilocytic astrocytoma. *J Neurosurg* 1988;69:171–176
9. Bilaniuk LT, Zimmerman RA, Littman P, et al. Computed tomography of brain stem gliomas in children. *Radiology* 1980;134: 89–95
10. Davis PC, Hoffman JC, Weidenheim KM. Large hypothalamic and optic chiasm gliomas in infants: difficulties in distinction. *AJNR* 1984;5:579–585
11. Aoki S, Barkovich AJ, Nishimura K, et al. Neurofibromatosis types 1 and 2: cranial MR findings. *Radiology* 1989;172:527–534
12. Geremia GK, Wollman R, Foust R. Computed tomography of gliomatosis cerebri. *J Comput Assist Tomogr* 1988;12:698–701
13. Spagnoli MV, Grossman RI, Packer RJ, et al. Magnetic resonance imaging determination of gliomatosis cerebri. *Neuroradiology* 1987;29:15–18
14. Barnard RO, Geddes JF. The incidence of multifocal cerebral gliomas: a histologic study of large hemisphere sections. *Cancer* 1987;60:1519–1531
15. Van Tassel P, Lee YY, Bruner JM. Synchronous and metachronous malignant gliomas: CT findings. *AJNR* 1988;9:725–732
16. Butler AR, Horii SC, Kricheff II, et al. Computed tomography in astroctyomas: a statistical analysis of the parameters of malignancy and the positive contrast-enhanced CT scan. *Radiology* 1978;129:433–439
17. Earnest F, Kelly PJ, Scheithauer BW, et al. Cerebral astroctyomas: histopathologic correlation of MR and CT contrast enhancement with stereotactic biopsy. *Radiology* 1988;166:823–827
18. Lee YY, Van Tassel P, Bruner JM, et al. Juvenile pilocytic astrocytomas: CT and MR characteristics. *AJNR* 1989;10: 363–370
19. Joyce P, Bentson J, Takehasin M, et al. The accuracy of predicting histologic grades of supratentorial astrocytomas on the basis of computerized tomography and cerebral angiography. *Neuroradiology* 1978;16:346–348
20. Steinhoff H, Lanksch W, Kazner E, et al. Computed tomography in the diagnosis and differential diagnosis of glioblastomas: a qualitative study of 295 cases. *Neuroradiology* 1977;14:193–200
21. Johnson PC, Hunt SJ, Drayer BP. Human cerebral gliomas: correlation of postmortem MR imaging and neuropathologic features. *Radiology* 1989;170:211–217
22. Atlas SW, Grossman RI, Gomori JM, et al. Calcified intracranial lesions: detection with gradient echo-acquisition rapid MR imaging. *AJNR* 1988;9:253–259
23. Dean BL, Drayer BP, Bird DR, et al. Gliomas: classification with MR imaging. *Radiology* 1990;174:411–415